

Impurity modelling with European Transport Simulator: implementation and verification

D. Yadykin¹, I. Ivanova-Stanik², T. Jonsson³, D. Coster⁴, K. Kirov⁵, D. Kalupin^{6,7}

¹ *Space, Earth and Environment, Chalmers University of Technology, Gothenburg, Sweden*

² *Institute of Plasma Physics and Laser Microfusion, Hery 23, 01-497 Warsaw, Poland*

³ *KTH, Royal Institute of Technology, Stockholm, Sweden*

⁴ *Max-Planck Institut für Plasmaphysik Garching, Germany*

⁵ *EUROfusion Consortium, JET, Culham Science Centre, Abingdon, OX14 3DB, UK*

⁶ *IEK-4 Plasmaphysik, Forschungszentrum Jülich GmbH, 52425 Juelich, Germany*

⁷ *EUROfusion PMU, Boltzmannstrasse 2, 85748 Garching, Germany*

Accurate modelling of the impurity evolution is an important part of the scenario modelling for the present and future fusion devices. Impurity effect on the plasma dynamics (like the impurity accumulation in the plasma core or the impurity effect on the power exhaust) should be included in the scenario modelling to get reliable predictions [1], [2].

European Transport Simulator (ETS) [3] is the integrated modelling tool (workflow) capable to interpret and predict scenarios of the fusion plasma devices. ETS includes several 'building' blocks describing different plasma processes (transport, heating, etc.) that are combined in transport equations describing evolution of the plasma profiles (poloidal flux, density, temperature). Equations for the evolution of the impurity densities are included in ETS. The verification of the impurity model for the ETS version using Consistent Physical Objects (CPOs) for the data transfer was reported in Recently, ETS is updated to use IMAS framework [4]. This was accompanied by the substantial modification of the impurity model implementation in the simulator.

Implementation in ETS

Equations for the evolution of the impurity densities are included in two versions of ETS (CPO based and IMAS based). The general idea of both implementation is the same: the density equations for the impurity species can be treated interpretively or evolved in giving the sources and the transport coefficients calculated for each charge state using ADAS data [5] provided through AMNS library. The boundary conditions and the initial profiles are provided at the configuration step of the workflow in the case when time evolution is activated. It is possible to use interpretive profiles or to apply coronal distribution. The density equations are written in generalized form (see reference) adopted in ETS to be used by all transport channels. Density

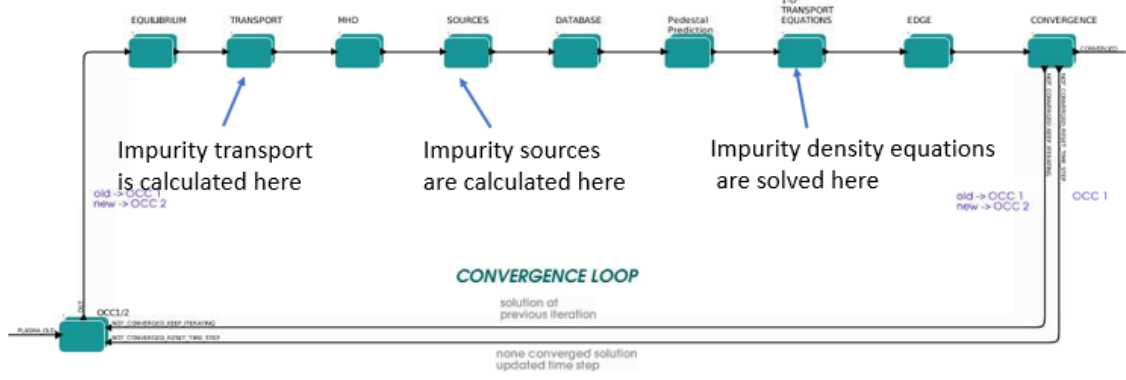


Figure 1: Kepler layout of the ETS Convergence Loop with indication of the modules relevant to the impurity density equations

equations are solved by the scheme proposed by K. Lakner [6] using two consequent iterations with half time step intervals and going up and down in the charge states on each half step. The implementation details though differ in the two ETS versions. This partially is caused by the adoption of the normalized radial coordinate ($x = \rho_{tor}/\rho_{tor}^a$ instead of ρ_{tor} in CPO based ETS version), where ρ_{tor} is the normalized toroidal flux, a - plasma minor radius. This allows for the

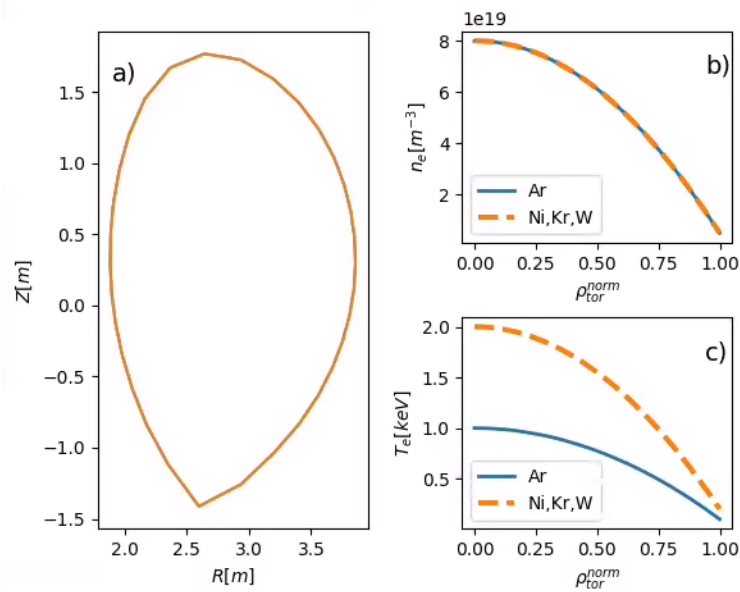


Figure 2: Input data used in the verification studies: a) plasma boundary; b) electron density; c) electron temperature. Solid - profiles used for Ar comparison, dashed - profiles used for Ni, Kr, W comparison.

moving plasma boundary that is important for the modelling of the transient discharge phases like ramp-up and ramp-down. Implementation logic is also modified in the IMAS based ETS version.

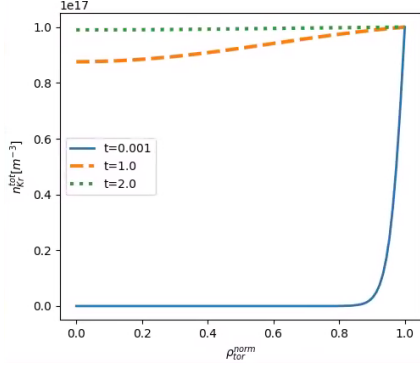


Figure 3: Evolution of the total density of the Kr during simulation time. Solid - after 1 ms; dashed - after 1 sec; dotted - after 2 sec.

Impurity equations are implemented in the source module in the CPO based version. Both the transport coefficients and the sources for the impurity density equations (ionization and recombination rates) are calculated in the same module. The numerical solver used to solve impurity density equation is prescribed and in general can be different to that used to solve for other channels. The implementation logic follows the general modular structure of the workflow for the IMAS based version of ETS. The density equations are solved in the same module as other channels (*TRANSPORT_EQUATIONS*) using the same numerical solver. The transport coefficients

and the source terms for the impurity density equations are calculated in the correspondent modules of ETS (*TRANSPORT* and *SOURCES* respectively) that are separated from the *TRANSPORT_EQUATIONS* module (see fig. 1).

Verification against the standalone simulation results

The verification of the impurity model for the ETS version using Consistent Physical Objects (CPOs) for the data transfer was reported in [7]. The verification of the ETS version based on the IMAS is also required as substantial modifications of the implementation were introduced (see above). The verification is done against the standalone simulations performed with SANCO code [8]. The evolution of the impurity density profile is followed for several impurity species (Ar, Ni, Kr, W) starting from the prescribed total density at the boundary. The boundary values of the charge state densities are taken from the results obtained with SANCO code. The diffusion coefficient profiles are set to be radially constant for all charge states with the diffusion coefficient value set to $D = 1.0 \text{ m}^2/\text{s}$. The sources (ionisation and recombination rates) are calculated using atomic data provided by the AMNS module. JET like geometry is used together with parabolic profiles of the electron/ion density and temperature. The value of on-axis electron density is chosen to be $n_e(0) = 8.0 \times 10^{19} \text{ m}^{-3}$ and the value of the on-axis electron temperature $T_e(0)$ is chosen to be 1 keV for Ar comparison and 2 keV for Ni, Kr, W comparison. Moreover, temperature equations are not solved and it is set $T_e = T_i$. The density of the main ion (D) is calculated from quasineutrality. The plasma boundary poloidal cross section and the kinetic profiles for electrons (n_e, T_e) are shown on fig. 2. The evolution of the total impurity density profile during the ETS simulation is shown on fig. 3 for Ar case. Density profile evolves similarly for other impurity species. The density of the selected impurity charge states, the radiation power

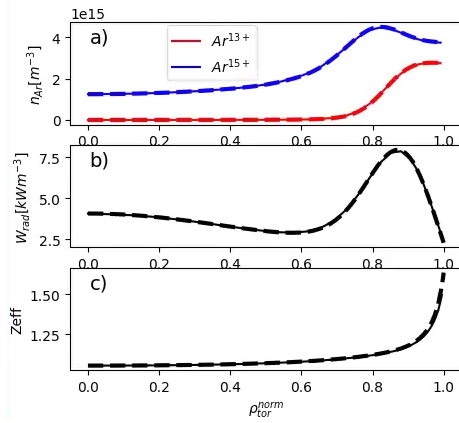


Figure 4: Results ETS/SANCO for Ar after 2 sec of simulation time. a) state densities; b) radiation power density; c) Z_{eff} . Solid - SANCO, dashed - ETS

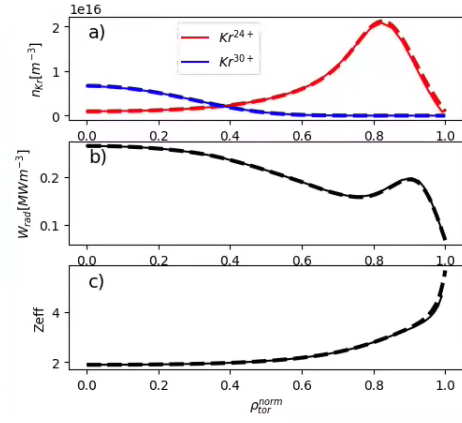


Figure 5: Results ETS/SANCO for Kr after 2 sec of simulation time. a) state densities; b) radiation power density; c) Z_{eff} . Solid - SANCO, dashed - ETS

density profile and the profile of effective charge are compared after 2 sec of the simulation time against the standalone results obtained with SANCO code for different impurity species. The comparison for Ar and W is shown on figs. 4,5. Good agreement between the ETS simulation and the standalone results is seen in both cases. This verifies the impurity implementation procedure adopted in ETS.

Acknowledgement

This work has been carried out within the framework of the EUROfusion Consortium, funded by the European Union via the Euratom Research and Training Programme (Grant Agreement No 101052200 — EUROfusion). Views and opinions expressed are however those of the author(s) only and do not necessarily reflect those of the European Union or the European Commission. Neither the European Union nor the European Commission can be held responsible for them.

References

- [1] Luda T. et al, Nucl. Fusion **60** (2020) 036023
- [2] Wischmeier M. et al, J. Nucl. Mat. **463** (2015) 22
- [3] Falchetto G. et al, P1-1081, 46th EPS conference, Milan, 2019
- [4] Imbeaux F. et al., Nucl. Fusion **55** (2015) 123006.
- [5] Summers H.P. The ADAS User Manual version, www.adas.ac.uk
- [6] Lackner K. et al., Z. Naturforsch. **37a** (1982) 931.
- [7] Kalupin D. et al., Nucl. Fusion **53** (2013) 123007
- [8] Lauro-Taroni L. et al., Proc. 21st EPS (1994) vol 1.